Journal of Fluorescence, Vol. 15, No. 2, March 2005 (© 2005)
DOI: 10.1007/s10895-005-2523-5

Effects of Refractive Index and Viscosity on Fluorescence and Anisotropy Decays of Enhanced Cyan and Yellow Fluorescent Proteins

Jan Willem Borst,[1] Mark A. Hink,[1] Arie van Hoek,[2] and Antonie J. W. G. Visser[1,3,4]

Received June 9, 2004; accepted October 9, 2004

The fluorescence lifetime strongly depends on the immediate environment of the fluorophore. Time-resolved fluorescence measurements of the enhanced forms of ECFP and EYFP in water–glycerol mixtures were performed to quantify the effects of the refractive index and viscosity on the fluorescence lifetimes of these proteins. The experimental data show for ECFP and EYFP two fluorescence lifetime components: one short lifetime of about 1 ns and a longer lifetime of about 3.7 ns of ECFP and for EYFP 3.4. The fluorescence of ECFP is very heterogeneous, which can be explained by the presence of two populations: a conformation (67% present) where the fluorophore is less quenched than in the other conformation (33% present). The fluorescence decay of EYFP is much more homogeneous and the amplitude of the short fluorescence lifetime is about 5%. The fluorescence anisotropy decays show that the rotational correlation time of both proteins scales with increasing viscosity of the solvent similarly as shown earlier for GFP. The rotational correlation times are identical for ECFP and EYFP, which can be expected since both proteins have the same shape and size. The only difference observed is the slightly lower initial anisotropy for ECFP as compared to the one of EYFP.

KEY WORDS: ECFP; EYFP; fluorescence lifetime; FLIM; FRET; rotational correlation time; refractive index; viscosity.

INTRODUCTION

The green fluorescent protein (GFP) isolated from the pacific jellyfish *Aequorea victoria*, its many colored variants and new fluorescent proteins from coral species are abundantly applied as genetically encoded markers in cell biology [1,2]. GFP and its variants are also widely used in various undergraduate and graduate courses organized in our universities (for an example see [3]). In this context, we have paid attention to one aspect of GFP-imaging that was published recently [4]. Briefly, it was demonstrated by fluorescence lifetime imaging microscopy (FLIM) of GFP that the fluorescence lifetime depends on the local refractive index. The main cause for this effect is that the radiative lifetime and the absorption and emission spectra of a fluorophore are dependent on the refractive index due to the polarizability of the medium surrounding the fluorophore. The Strickler–Berg formula describes the relationship between the radiative lifetime, the absorption spectrum of the fluorophore, the third moment of the fluorescence spectrum and the square of the refractive index [5]. Toptygin *et al*. [6] performed a detailed study of the refractive index effect on the radiative decay rate of a single tryptophan in a protein and showed that the theoretical prediction agrees with the experimental data. These authors derived a more complex model than the Strickler–Berg equation with a dependence

[1] Laboratory of Biochemistry, MicroSpectroscopy Centre, Wageningen University, Dreijenlaan 3, 6703 HA Wageningen, The Netherlands.
[2] Laboratory of Biophysics, MicroSpectroscopy Centre, Wageningen University, Dreijenlaan 3, 6703 HA Wageningen, The Netherlands.
[3] Department of Structural Biology, Faculty of Earth and Life Sciences, Vrije Universiteit, De Boelelaan 1087, 1081 HV Amsterdam, The Netherlands.
[4] To whom correspondence should be addressed. E-mail: Ton.Visser@wur.nl

of the inverse radiative lifetime on the power of the refractive index in excess of 2 [6]. Suhling *et al.* [4] studied the fluorescence decay of GFP in different solvents and in glycerol–water mixtures (0–90%) and found that the inverse of the average lifetime scales linearly with the square of the refractive index. Alternatively, by using FLIM experiments these authors could then also image the refractive index of the environment of GFP. The observations may have implications for FLIM measurements of fluorescent proteins in cells. In cells the refractive index can adopt a range of values varying from 1.45 to 1.6 in membrane environments to 1.35 in the cytoplasm.

The cyan fluorescent protein (CFP, donor) and the yellow fluorescent protein (YFP, acceptor) are frequently used as donor–acceptor pairs in Förster resonance energy transfer (FRET) studies for the investigation of protein–protein interactions in cells. Especially for FLIM measurements reporting on FRET we need to know the fluorescence lifetime of the donor in the absence of acceptor. This would imply that these reference lifetimes depend on the local refractive index and will be different in either membrane- or cytosolic environments of the cell. This prompted us to study the time-resolved fluorescence properties of the enhanced forms of CFP and YFP (ECFP and EYFP, respectively) in water–glycerol mixtures. Since glycerol is much more viscous than water, we also study the fluorescence anisotropy decays of the same samples. From these experiments we determine the rotational correlation time of both proteins and show that the rotational correlation time scales with increasing viscosity of the solvent similarly as shown earlier for GFP [7].

THEORETICAL BACKGROUND

Time-Resolved Fluorescence

The fluorescence lifetime τ is the time a fluorophore remains in its excited state after excitation and is related to the radiative (k_r) and nonradiative (k_{nr}) rate constants:

$$\tau = \frac{1}{k_r + k_{\mathrm{nr}}} \tag{1}$$

The fluorescence lifetime strongly depends on the immediate environment of the fluorophore and can therefore be used as a sensor for environment. There exists a fundamental relationship between the fluorescence lifetime τ and the fluorescence quantum yield Q:

$$Q = \frac{\tau}{\tau_r} = \frac{k_r}{k_r + k_{\mathrm{nr}}} \tag{2}$$

in which $\tau_r(=1/k_r)$ is the radiative lifetime of the fluorescent molecule. The radiative lifetime can be visualized as that lifetime of the excited state when the only deactivation process consists of photon emission. One of the empirical relationships between τ_{r} and a light absorption spectrum is that derived by Strickler and Berg [5]:

$$\frac{1}{\tau_r} = 2.88 \times 10^{-9}\, n^2 \frac{\int I(\sigma)\, d\sigma}{\int I(\sigma)\sigma^{-3} d\sigma} \int \frac{\varepsilon(\sigma)}{\sigma}\, d\sigma \tag{3}$$

in which n is the refractive index, I the fluorescence emission, ε the molar extinction coefficient connected with the first (lowest) electronic transition and σ the wavenumber. The Strickler–Berg equation strictly applies to the natural fluorescence lifetime (τ_r). However, Suhling *et al.* [4] found no distinct effect of the quantum yield of GFP fluorescence on the refractive index, whereas a clear dependence of the inverse actual lifetime on the quadratic refractive index is observed.

Time-Resolved Fluorescence Anisotropy

The experimental observable in a time-resolved fluorescence anisotropy experiment defined as:

$$r(t) = \frac{I_{\parallel}(t) - I_{\perp}(t)}{I_{\parallel}(t) + 2I_{\perp}(t)} \tag{4}$$

where $I_{\parallel}(t)$ and $I_{\perp}(t)$ are the observed time-dependent parallel and perpendicular polarized components relative to the polarization direction of the exciting beam. The general expression relating the experimental anisotropy $r(t)$ with the time-dependent correlation function of the transition moments has the form of a second-order Legendre polynomial $P_2(x)$ [8]:

$$r(t) = \langle P_2[\mu_{\mathrm{a}}(0) \cdot \mu_{\mathrm{e}}(t)] \rangle \tag{5}$$

where $\mu_{\mathrm{a}}(0)$ and $\mu_{\mathrm{e}}(t)$ are unit vectors along the absorption transition moment at time zero (note that light absorption is a femtosecond process) and emission at time t after excitation, respectively. The brackets $\langle\ \rangle$ denote an ensemble average. In proteins there are several contributions to the loss of anisotropy [9]. In case of GFP the main sources of depolarization are an intrinsic one leading to the fundamental anisotropy (the anisotropy at time zero) and protein tumbling, since the fluorophore is rigidly embedded within the protein matrix [7,10,11]. The fundamental anisotropy contains information about the angle θ between absorption and emission transition moments:

$$r(0) = \frac{2}{5}\left(\frac{3\ \cos^2\theta - 1}{2}\right) \tag{6}$$

Note that $r(0) = 0.4$ corresponds with parallel absorption and emission dipoles ($\theta = 0^\circ$). For an spherically shaped protein with firmly attached fluorophore the anisotropy

decays mono-exponentially with a characteristic rotational correlation time ϕ:

$$r(t) = r(0)e^{-t/\phi} \tag{7}$$

The rotational correlation time ϕ is proportional to the viscosity η and the molecule volume V according to the Stokes–Einstein relationship:

$$\phi = \frac{\eta V}{kT} \tag{8}$$

where k is the Boltzmann constant and T the absolute temperature.

MATERIALS AND METHODS

The enhanced forms of CFP and YFP were isolated as described in [12].

The glycerol mixtures (0, 10, 30, 50, 70 and 90% v/v) were prepared by mixing glycerol, (Merck: spectroscopic grade) with phosphate buffered saline pH 7.4 (PBS). The purified proteins ECFP and EYFP were diluted to a final concentration of 200 nM.

Time-resolved fluorescence measurements were carried out using mode-locked continuous wave lasers for excitation and time-correlated photon counting as detection technique. The pump laser was a CW diode-pumped, frequency-doubled Nd:YVO_4 laser (Coherent Inc., Santa Clara, CA, model Verdi V10). The mode-locked laser was a titanium:sapphire laser (Coherent Inc., Santa Clara, CA, model Mira 900-D in fs mode), tuned to 860 nm for CFP and 960 nm for EYFP. At the output of the titanium:sapphire laser a pulse picker was placed (APE GmbH, Berlin, Germany, model Pulse Select), decreasing the repetition rate of excitation pulses to 3.8×10^6 pulses per second. The output of the pulse picker was directed towards a frequency doubler (Inrad Inc., Northvale, NJ, model 5-050, Ultrafast Harmonic Generation System). For excitation maximum pulse energy of sub-pJ was used, the wavelength was 430 nm for CFP and 480 for EYFP and the pulse duration about 0.2 ps.

The samples were in 1.5 mL and 10 mm light path fused silica cuvettes (Hellma GmbH, Müllheim, Germany, model 111-QS), placed in a sample holder, temperature controlled (20°C) by applying thermoelectric (Peltier) elements and a controller (Marlow Industries Inc., Dallas, TX, model SE 5020). The sample holder was placed in a housing also containing the main detection optics. Extreme care was taken to avoid artifacts from depolarization effects. At the front of the sample housing a Glan-laser polarizer was mounted, optimizing the already vertical polarization of the input light beam. The fluorescence was collected at an angle of 90° with respect to the direction of the exciting light beam. Between the sample and the photomultiplier detector were placed a single fast lens (uncoated fused silica, F/3.0), cut-off filters KV470 for ECFP and OG515 for EYFP (both filters are from Schott, Mainz, Germany), a rotatable sheet type polarizer and a second single fast lens (uncoated fused silica, F/3.0), focusing the fluorescence on the photomultiplier cathode. The polarizer sheet was in a dc motor driven ball-bearing holder with mechanical stops, allowing computer-controlled rotation (0.2 s) to parallel and perpendicular polarized detection of emission. The sheet polarizer was Polaroid type HNP'B. The polarizers were carefully aligned and the performance of the setup finally checked by measuring reference samples.

Detection electronics were time-correlated single photon counting modules. With a small portion of the mode-locked light at 860 nm (or 960 nm) wavelength, left from the harmonics conversion, a fast PIN-photodiode (Hewlett Packard Inc., Palo Alto, CA, model 5082-4204 at 45 V reverse bias) was excited. The output pulses of this photodiode were fed to one channel of a quad constant fraction discriminator (CFD, Tennelec Inc., Oak Ridge, TS, modified model TC 454), and then used as stop signal for a time-to-amplitude converter (TAC, Tennelec Inc., Oak Ridge, TS, model TC 864). A microchannel plate photomultiplier (Hamamatsu, Hamamatsu, Japan, model R3809U-50 at 3100 V, cooled down by a water bath to a few degrees centigrade) was used for the detection of the fluorescence photons. The single photon responses of this PMT were amplified by a wide-band amplifier (Becker & Hickl GmbH, Berlin, Germany, model ACA-2; 21 dB, 1.8 GHz), analyzed in another channel of the CFD and then used as a start signal for the TAC. The output pulses of the TAC were analyzed by an analogue-to-digital converter (ADC, Nuclear Data Inc., Schaumburg, IL, model 8715, 800 ns fixed dead-time), used in Coincidende and Sampled Voltage Analysis mode, gated by the Valid Conversion Output of the TAC. The output of the ADC was gathered in 4096 channels of a multichannel analyzer (MCA board from Nuclear Data Inc., Schaumburg, IL, model AccuspecB, in a personal computer). The channel time spacing was 5.0 ps.

By reducing the energy of the excitation pulses with neutral density filters, the rate of fluorescence photons was decreased to less than 30,000 per second (≈1% of 3.8 MHz [13]), to prevent pile-up distortion. Also other instrumental sources for distortion of data were minimized [14] to below the noise level of normal photon statistics. Measurements consisted of repeated sequences of measuring during 10 s parallel and 10 s perpendicular polarized emissions. After measuring the fluorescence of the

sample, the background emission of the buffer solution was measured and used for background subtraction.

For obtaining a dynamic instrumental response of the experimental setup the single exponential fluorescence decay of erythrosine B in water (90 ps) was recorded. One complete experiment for a fluorescence decay measurement consisted of the recording of data sets of the reference compound, the unknown sample, the background (buffer) fluorescence and again the reference compound.

Data analysis was performed using a model of discrete exponential terms. Global fitting of the experimental data was performed using the 'TRFA Data Processing Package' of the Scientific Software Technologies Center (Belarusian State University, Minsk, Belarus) [15].

The total fluorescence intensity decay $I(t)$ and anisotropy decay $r(t)$ are obtained from the measured parallel $I_{\parallel}(t)$ and perpendicular $I_{\perp}(t)$ fluorescence intensity components through the relations:

$$I(t) = I_{\parallel}(t) + 2gI_{\perp}(t) \tag{9}$$

$$r(t) = \frac{I_{\parallel}(t) - gI_{\perp}(t)}{I_{\parallel}(t) - 2gI_{\perp}(t)} \tag{10}$$

in which the g-factor describes the sensitivity of the detection system for the perpendicular component with respect to the parallel one. For the setup used the g-factor equals unity [16] leading to the same expression as Eq. 4. The fluorescence lifetime profile consisting of a sum of discrete exponentials with lifetime τ_i and amplitude α_i can be retrieved from the total fluorescence $I(t)$ through the convolution product with the instrumental response function $E(t)$:

$$I(t) = E(t) \otimes \sum_{i=1}^{N} \alpha_i e^{-t/\tau_i} \tag{11}$$

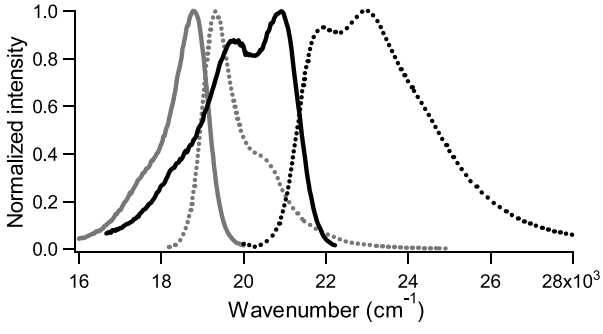

Fig. 1. Fluorescence excitation (dotted) and emission (solid) spectra of ECFP (black) and EYFP (gray) in PBS (pH 7.4) on wavenumber scale.

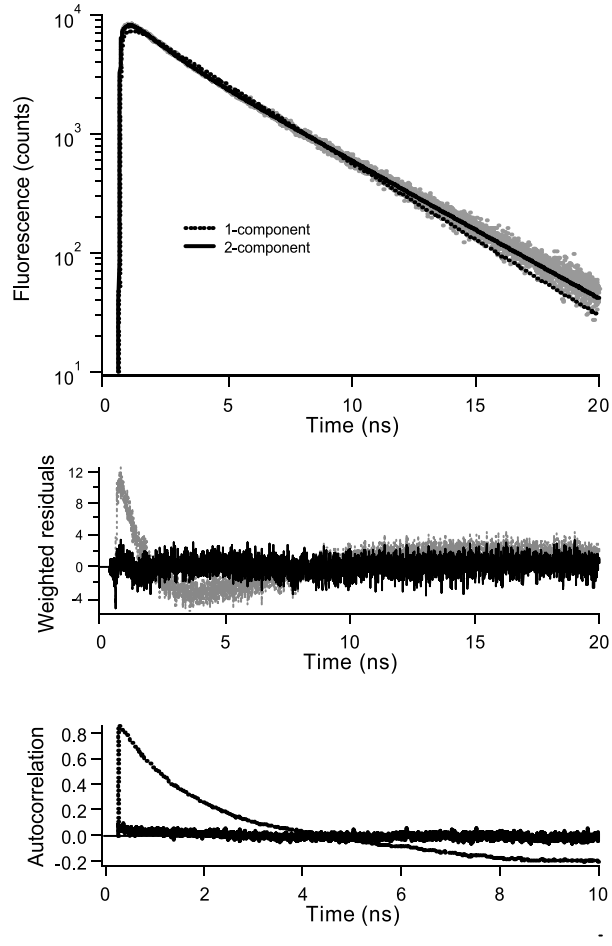

Fig. 2. Fluorescence decay analysis of ECFP in PBS (pH 7.4) using one lifetime component (dotted) or two lifetime components (solid). The weighted residuals between experimental and calculated points and the autocorrelation of the residuals clearly illustrate the superior fit with two lifetimes (black traces). One-exponential fit: $\tau = 3.34$ ns, $\chi^2 = 6.8$. Two-exponential fit: $\alpha_1 = 0.335, \tau_1 = 1.14, \alpha_2 = 0.665, \tau_2 = 3.72$, $\chi^2 = 1.12$. A three-exponential fit gave a slight improvement with a sub-nanosecond lifetime of small amplitude and $\chi^2 = 1.07$ (results not shown).

Fluorescence lifetime analysis of the enhanced forms of CFP and YFP required a two-component model ($N = 2$) for optimal fitting.

In fluorescence anisotropy analysis, after deconvolution the time-dependent fluorescence anisotropy $r(t)$ is calculated from the parallel and perpendicular intensity components through the relations [9]:

$$I_{\parallel}(t) = \frac{1}{3}\sum_{i=1}^{N} \alpha_i e^{-t/\tau_i}[1 + 2r(0)e^{-t/\phi}] \tag{12}$$

$$I_{\perp}(t) = \frac{1}{3}\sum_{i=1}^{N} \alpha_i e^{-t/\tau_i}[1 - r(0)e^{-t/\phi}] \tag{13}$$

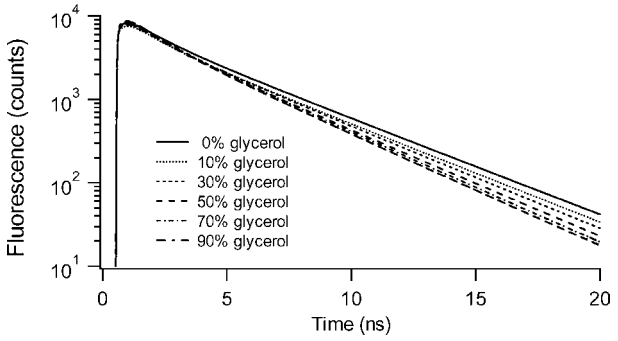

Fig. 3. Calculated fluorescence decays of ECFP in different water–glycerol mixtures obtained after global analysis linking the shorter lifetime. Analysis results are collected in Table I.

Global analysis [17], in which data sets were fitted simultaneously with a sum of discrete exponentials, was performed by linking common fluorescence lifetimes for multiple data sets. In addition, a rigorous error analysis at the 67% confidence level was applied to the optimized fluorescence lifetimes and rotational correlation times.

RESULTS AND DISCUSSION

Excitation and Fluorescence Spectra on Wavenumber Scale

The corrected, normalized excitation and emission spectra of ECFP and EYFP in water on wavenumber scale are presented in Fig. 1. In case of ECFP the fine structure of excitation and emission bands can be clearly distinguished. This fine structure originates from vibrational transitions superimposed on the single electronic transition [1,12]. The spectra and the maximum extinction coefficients are taken as described previously [3]. The radiative lifetimes of the fluorescence of ECFP and EYFP are calculated as 5.0 and 7.2 ns, respectively. Since the absorption and emission spectra of both proteins do not change upon a change of refractive index (data not shown), the use of Eq. 3 allows calculating the radiative lifetime as function of refractive index.

Fluorescence Decays in Different Water–Glycerol Mixtures

The total fluorescence decay of ECFP in aqueous solution is shown in Fig. 2. These experimental data could not be fitted with a single exponential component, but needed (at least) two lifetime components for an optimal fit. One shorter lifetime of 1.1 ns contributing for 33% and one longer lifetime of 3.7 ns contributing for 67% could be recovered. The departure of single-exponential fluorescence decay is also observed by others [18–20]. The presence of multiple fluorescent states is most probably due to two different conformations of ECFP in the crystal structure in which two amino acids, Tyr145 and His148, are positioned differently with respect to the fluorophore [21]. The heterogeneity of ECFP fluorescence can be explained by the presence of two populations: a conformation (67% present) where the fluorophore is less quenched than in the other conformation (33% present). The interconversion between both conformations is slow on the fluorescence time scale. From site-directed mutagenesis studies, His148 has been found to be the major quencher of the fluorophore [19].

Addition of increasing amounts of glycerol did not change the heterogeneous fluorescence decay pattern. The short lifetime does not change, whereas the long lifetime becomes progressively shorter at higher glycerol concentration (or higher refractive index of the solvent). Since the short lifetime is hardly influenced, we have performed a global analysis of six decay curves linking the short lifetime and leaving the fluorescence lifetime of the longer component as an adjustable parameter. The fitted curves are presented in Fig. 3. The plots of weighted residuals and

Table I. Effect of Refractive Index Changes on the Fluorescence Decay Parameters of ECFP in Glycerol

	Refractive index (n)	α_1	τ_1 (ns)	α_2	τ_2 (ns)	$\langle\tau\rangle$ (ns)
0% glycerol	1.33	0.335	1.14 (1.07–1.20)	0.665	3.72 (3.65–3.77)	2.86
10% glycerol	1.34	0.35	1.14 (1.07–1.20)	0.65	3.65 (3.58–3.69)	2.77
30% glycerol	1.37	0.35	1.14 (1.07–1.20)	0.65	3.50 (3.46–3.54)	2.67
50% glycerol	1.40	0.35	1.14 (1.07–1.20)	0.65	3.34 (3.32–3.42)	2.57
70% glycerol	1.43	0.36	1.14 (1.07–1.20)	0.64	3.22 (3.19–3.28)	2.48
90% glycerol	1.46	0.40	1.14 (1.07–1.20)	0.60	3.19 (3.15–3.24)	2.37

Note. Values in parentheses are the 67% confidence limits. The average lifetime is calculated as $\langle\tau\rangle = \alpha_1\tau_1 + \alpha_2\tau_2$.

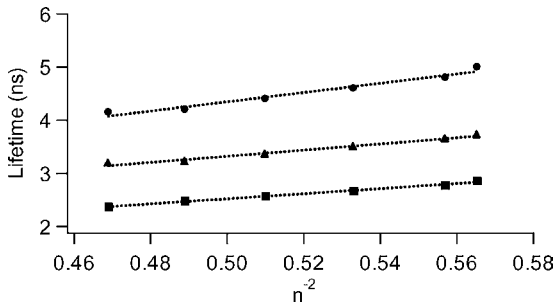

Fig. 4. Fluorescence lifetimes of ECFP in different water–glycerol mixtures as a function of the inverse of the squared refractive index. Radiative lifetime: •; long lifetime: ▲; average lifetime: ■.

autocorrelation of the residuals are similar compared to the ones presented for the two-component fit in Fig. 2. All parameters (amplitudes and lifetimes), confidence limits of the lifetimes and the average lifetimes ($\langle\tau\rangle$) are collected in Table I. The long decay time, the average fluorescence lifetime and calculated radiative lifetime are plotted against the inverse quadratic refractive index (n^{-2}) in Fig. 4. Both experimental lifetimes show a linear relationship similarly as found for GFP [4]. Therefore, also ECFP shows a fluorescence decay that is sensitive to its immediate environment. In addition, it is verified that the fluorescence quantum yield (see Eq. 2) of ECFP is indeed independent of refractive index as has been experimentally shown for GFP [4].

Similar fluorescence decay experiments in different glycerol–water mixtures were performed for EYFP. For EYFP in PBS a one-component fit yielded a lifetime of 3.34 ns ($\chi^2 = 1.20$). A slightly better fit ($\chi^2 = 1.13$) to the experimental data is obtained with two fluorescence lifetime components: one short lifetime of 0.85 ns and a longer lifetime of 3.37 ns of EYFP in aqueous solution. However, the amplitude of the short lifetime is much smaller (4%) than the one of the long lifetime (96%), making the fluorescence decay of EYFP much more homogeneous. A global analysis of six decay curves for different glycerol–water mixtures linking the short lifetime has been performed as well. All fit parameters are collected in Table II. Because of its small amplitude, the short lifetime is less defined than in case of ECFP. Plots of the long and average fluorescence lifetimes of EYFP against n^{-2} are more coincident than for ECFP and, together with that of the radiative lifetime, show a linear relationship as well (Fig. 5).

Fluorescence Anisotropy Decays in Different Water–Glycerol Mixtures

Experimental and fitted fluorescence anisotropies of ECFP in water and 30% glycerol–water mixtures are shown in Fig. 6. The weighted residuals and autocorrelation plots are randomly distributed around zero illustrating the good quality of the fits (results not shown). Only within this range of viscosity values the rotational correlation times can be accurately determined. When the relative viscosity becomes too high (>6), the anisotropy is decaying too slowly in the available time window of the experiments (20 ns) leading to inaccurate rotational correlation times with undefined confidence limits. The recovered rotational correlation times are plotted against the relative viscosity in Fig. 7. It can be clearly seen that there is a linear relationship as predicted by the Stokes–Einstein equation (Eq. 8). In addition, the confidence limits become larger at longer correlation times in agreement with the aforementioned explanation. The fluorescence anisotropy data of EYFP show the same tendencies as observed for those of ECFP. The rotational correlation times, the confidence limits and initial amplitudes determined from the analysis of time-dependent anisotropies of ECFP and EYFP at four relative viscosities are collected in Table III. The rotational correlation times are identical for ECFP and EYFP, which can be expected since both proteins are the same. The only difference arises from a different fundamental anisotropy that is slightly lower

Table II. Effect of Refractive Index Changes on the Fluorescence Decay Parameters of EYFP in Glycerol

	Refractive index (n)	α_1	τ_1 (ns)	α_2	τ_2 (ns)	$\langle\tau\rangle$ (ns)
0% glycerol	1.33	0.043	1.06 (0.71–1.54)	0.957	3.37 (3.31–3.41)	3.27
10% glycerol	1.34	0.030	1.06 (0.71–1.54)	0.970	3.25 (3.19–3.29)	3.18
30% glycerol	1.37	0.057	1.06 (0.71–1.54)	0.943	3.15 (3.09–3.19)	3.03
50% glycerol	1.40	0.032	1.06 (0.71–1.54)	0.968	3.01 (2.95–3.05)	2.95
70% glycerol	1.43	0.053	1.06 (0.71–1.54)	0.947	2.89 (2.86–2.96)	2.79
90% glycerol	1.46	0.152	1.06 (0.71–1.54)	0.848	2.74 (2.66–2.83)	2.48

Note. Values in parentheses are the 67% confidence limits. The average lifetime is calculated as $\langle\tau\rangle = \alpha_1\tau_1 + \alpha_2\tau_2$.

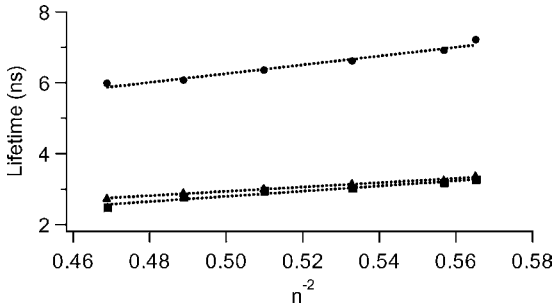

Fig. 5. Fluorescence lifetimes of EYFP in different water–glycerol mixtures as a function of the inverse of the squared refractive index. Radiative lifetime: •; long lifetime: ▲; average lifetime: ■.

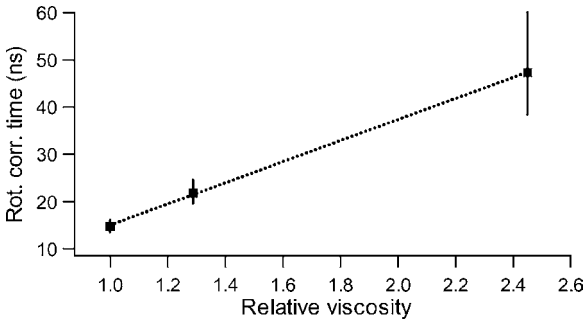

Fig. 7. Plot of rotational correlation time ϕ against relative viscosity for three water–glycerol mixtures (0, 10 and 30% glycerol, respectively). The confidence limits are also plotted in the same graph.

for ECFP ($\beta = 0.356 \pm 0.004$) as compared to EYFP ($\beta = 0.382 \pm 0.002$). This is probably caused by a different angle between absorption and emission moments in both chromophores. By using Eq. 6, these angles are $\theta = 16^\circ$ for ECFP and $\theta = 10^\circ$ for EYFP.

CONCLUDING REMARKS

We have shown that the fluorescence lifetimes of ECFP and EYFP are dependent on the refractive index of the medium. In the range of refractive index values 1.33–1.46 the average lifetimes decrease from 2.9 to 2.4 ns for ECFP and from 3.3 to 2.5 ns for EYFP. Provided that the accuracy of FLIM measurements is sufficiently high, these lifetime changes should be measurable in living cells allowing imaging of relative refractive index changes. EYFP should then be preferably used, since the relative change in lifetime is larger and the fluorescence decay is largely single exponential.

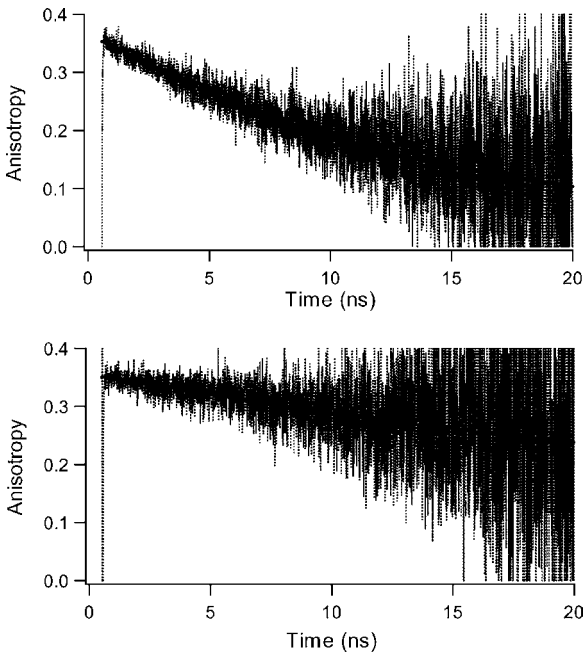

Fig. 6. Experimental and fitted fluorescence anisotropy decays of ECFP in water (PBS, pH 7.4) (top panel) and in a mixture of 70% water and 30% glycerol (lower panel). The recovered anisotropy parameters are listed in Table III.

Some caution is necessary for FLIM measurements reporting on FRET when ECFP is the donor, since the fluorescence decay is clearly non-exponential having a relatively long lifetime of 3.7 ns (67% present) and a relatively short lifetime of 1.1 ns (33% present). In FLIM experiments using single-photon timing, fluorescence decays are usually obtained with much less photons collected in the peak than for the cuvette experiment shown in Fig. 2. The ECFP-lifetime values obtained in the absence of acceptor are usually in the range of the average lifetimes 2.5–2.7 ns corresponding to refractive indices characteristic for cellular environments [22]. When one uses the average lifetime in case of FRET to calculate the transfer efficiency, one important assumption is that both lifetimes must equally reflect the rate of energy transfer. For example, when the transfer efficiency is 50%, then the short lifetime must be reduced from 1.14 to 0.57 ns and the longer one from 3.5 to 1.75 ns, yielding an average fluorescence lifetime of 1.34 ns as compared to 2.67 ns in the absence of FRET (see Table I). In order to eliminate the environment-sensitive lifetime of ECFP in FLIM experiments reporting on FRET, acceptor photobleaching should then be applied yielding a reference donor fluorescence lifetime [23]. Again, because of its mono-exponential fluorescence decay, EYFP would be a much better donor in FLIM experiments reporting on FRET.

The anisotropy decays of ECFP and EYFP accurately reports on the protein rotational motion when the

Table III. Anisotropy Decay Parameters of ECFP and EYFP in Different Water–Glycerol Mixtures

Solution	Relative viscosity	ECFP β	ECFP ϕ (ns)	EYFP β	EYFP ϕ (ns)
0% glycerol	1.00	0.353	14.8 (13.5–16.2)	0.381	15.6 (14.2–17.1)
10% glycerol	1.29	0.359	21.8 (19.6–24.7)	0.383	22.5 (19.8–25.7)
30% glycerol	2.45	0.351	47.4 (38.4–60.3)	0.382	47.7 (39.5–60.5)
50% glycerol	6.0	0.362	78 (56–123)	0.384	120 (75–n.f.)

Note. Values in parentheses are the 67% confidence limits. n.f.: upper confidence limit could not be found.

macroscopic viscosity is up to 2.5 larger than that of water. The average fluorescence lifetime is too short to report on slower rotations in higher-viscosity media. The initial anisotropy of ECFP is significantly lower than that of EGFP and EYFP.

ACKNOWLEDGMENT

This work was supported by an investment grant from the Council for Earth and Life Sciences of The Netherlands Organization for Scientific Research.

REFERENCES

1. R. Y. Tsien (1998). The green fluorescent protein. *Annu. Rev. Biochem.* **67**, 509–544.
2. A. Miyawaki, A. Sawano, and T. Takako (2003). Lighting up cells: Labeling proteins with fluorophores. *Suppl. Nature Cell Biol.* **5**, S1–S7.
3. M. A. Hink, N. V. Visser, J. W. Borst, A. van Hoek, and A. J. W. G. Visser (2003). Practical use of corrected fluorescence excitation and emission spectra of fluorescent proteins in Förster Resonance Energy Transfer (FRET) studies. *J. Fluoresc.* **13**, 185–188.
4. K. Suhling, J. Siegel, D. Phillips, P. M. W. French, S. Lévêque-Fort, S. E. D. Webb, and D. M. Davis (2002). Imaging the environment of green fluorescent protein. *Biophys. J.* **83**, 3589–3595.
5. S. J. Strickler and R. A. Berg (1962). Relationship between absorption intensity and fluorescence lifetime of molecules. *J. Chem. Phys.* **37**, 814–820.
6. D. Toptygin, R. S. Savtchenko, N. D. Meadow, S. Roseman, and L. Brand (2002). Effect of solvent refractive index on the excited-state lifetime of a single tryptophan residue in a protein. *J. Phys. Chem. B.* **106**, 3724–3734.
7. K. Suhling, D. M. Davis, and D. Phillips (2002). The influence of solvent viscosity on the fluorescence decay and time-resolved anisotropy of green fluorescent protein. *J. Fluoresc.* **12**, 91–95.
8. A. Szabo (1984) Theory of fluorescence depolarization in macromolecules and membranes. *J. Chem. Phys.* **81**, 150–167.
9. J. R. Lakowicz (1999). *Principles of Fluorescence Spectroscopy*, 2nd ed., Kluwer Academic/Plenum Publishers, New York.
10. M. A. Uskova, J. W. Borst, A. van Hoek, A. Schots, N. L. Klyachko, and A. J. W. G. Visser (2000). Fluorescence dynamics of green fluorescent proteins in AOT reversed micelles. *Biophys. Chem.* **87**, 73–84.
11. A. Volkmer, V. Subramanian, D. J. S. Birch, and T. M. Jovin (2000). One- and two-photon excited fluorescence lifetimes and anisotropy decays of green fluorescent proteins. *Biophys. J.* **78**, 1589–1598.
12. N. V. Visser, M. A. Hink, J. W. Borst, G. N. M. van der Krogt, and A. J. W. G. Visser (2002). Circular dichroism spectroscopy of fluorescent proteins. *FEBS Lett.* **521**, 31–35.
13. K. Vos, A. van Hoek, and A. J. W. G. Visser (1987). Application of a reference deconvolution method to tryptophan fluorescence in proteins. A refined description of rotational dynamics. *Eur. J. Biochem.* **165**, 55–63.
14. A. van Hoek and A. J. W. G. Visser (1985). Artefact and distortion sources in time correlated single photon counting. *Anal. Instrum.* **14**, 359–378.
15. A. V. Digris, V. V. Skakun, E. G. Novikov, A. van Hoek, A. Claiborne, and A. J. W. G. Visser (1999). Thermal stability of a flavoprotein assessed from associative analysis of polarized time-resolved fluorescence spectroscopy. *Eur. Biophys. J.* **28**, 526–531.
16. A. van Hoek, K. Vos, and A. J. W. G. Visser (1987). Ultrasensitive time-resolved polarized fluorescence spectroscopy as a tool in biology and medicine. *IEEE J. Quant. Electron.* **QE-23**, 1812–1820.
17. J. M. Beechem, E. Gratton, M. Ameloot, J. R. Knutson, and L. Brand (1991). The global analysis of fluorescence intensity and anisotropy decay data: Second generation theory and programs. in J. R. Lakowicz (Ed.), *Topics in Fluorescence Spectroscopy*, Plenum Press, New York, pp. 241–305.
18. M. Tramier, I. Gautier, T. Piolot, S. Ravalet, K. Kemnitz, J. Coppey, C. Durieux, V. Mignotte, and M. Coppey-Moisan (2002). Picosecond-hetero-FRET microscopy to probe protein–protein interactions in live cells. *Biophys. J.* **83**, 3570–3577.
19. M. A. Rizzo, G. H. Springer, B. Granada, and D. W. Piston (2004). An improved cyan fluorescent protein variant useful for FRET. *Nature Biotechnol.* **22**, 445–449.
20. S. Habuchi, M. Cotlet, J. Hofkens, G. Dirix, J. Michiels, J. Vanderleyden, V. Subramanian, and F. C. De Schryver (2002). Resonance energy transfer in a calcium concentration-dependent cameleon protein. *Biophys. J.* **83**, 3499–3506.
21. J. Hyun Bae, M. Rubini, G. Jung, G. Wiegand, M. H. J. Seifert, M. K. Azim, J.-S. Kim, A. Zumbusch, T. A. Holak, L. Moroder, R. Huber, and N. Budisa (2003). Expansion of the genetic code enables design of a novel "gold" class of green fluorescent proteins. *J. Mol. Biol.* **328**, 1071–1081.
22. J. W. Borst, M. A. Hink, A. van Hoek, and A. J. W. G. Visser (2003). Multiphoton microspectroscopy in living plant cells. *Proc. SPIE* **4963**, 231–238.
23. F. S. Wouters, P. J. Verveer, and P. I. H. Bastiaens (2001). Imaging biochemistry inside cells. *Trends Cell Biol.* **11**, 203–210.